Reconfiguration of brain network architecture to support executive control in aging

Courtney L. Gallen [a,*], Gary R. Turner [b], Areeba Adnan [b], Mark D'Esposito [a,c]

[a] Helen Wills Neuroscience Institute, University of California, Berkeley, CA, USA
[b] Department of Psychology, Sherman Health Sciences Research Centre, York University, Toronto, Ontario, Canada
[c] Department of Psychology, University of California, Berkeley, CA, USA

ARTICLE INFO

ABSTRACT

Aging is accompanied by declines in executive control abilities and changes in underlying brain network architecture. Here, we examined brain networks in young and older adults during a task-free resting state and an N-back task and investigated age-related changes in the modular network organization of the brain. Compared with young adults, older adults showed larger changes in network organization between resting state and task. Although young adults exhibited increased connectivity between lateral frontal regions and other network modules during the most difficult task condition, older adults also exhibited this pattern of increased connectivity during less-demanding task conditions. Moreover, the increase in between-module connectivity in older adults was related to faster task performance and greater fractional anisotropy of the superior longitudinal fasciculus. These results demonstrate that older adults who exhibit more pronounced network changes between a resting state and task have better executive control performance and greater structural connectivity of a core frontal-posterior white matter pathway.

© 2016 Elsevier Inc. All rights reserved.

1. Introduction

Cognitive decline is pervasive in older adulthood, notably in executive control processes thought to be subserved by the frontal cortex (Grady, 2008, 2012; Park et al., 2002). Extensive alterations in brain structure and function are also observed in older adults. Functional changes in aging have been documented in the activation of individual brain regions and in the functional connectivity between brain regions (Grady, 2012; Spreng et al., 2010; Turner and Spreng, 2012, 2015). Alterations in functional connectivity are thought to be related, in part, to a decline in structural connectivity, such as through long-range white matter fiber tracts (Bennett and Madden, 2014).

Further work in older adults has examined the functional communication among groups of brain regions by quantifying the connectivity of brain subnetworks (Andrews-Hanna et al., 2007; Damoiseaux et al., 2008; Ferreira and Busatto, 2013), such as the default-mode and fronto-parietal networks. However, executive control processes rely on the integration of signals from frontal cortex to widely distributed brain regions, likely not limited to specific subnetworks as has been examined thus far (Barceló et al., 2000; Chao and Knight, 1998; Fuster et al., 1985; Knight et al., 1999; Lee and D'Esposito, 2012; Miller and D'Esposito, 2005). Thus, changes in executive control processing in aging may be better examined by methods that quantify the large-scale (e.g., whole brain) network organization of the brain. Graph theoretical methods describe the brain as a complex network, comprised of functionally separable subnetworks or modules. This type of organization is critical for supporting both local processing within and global processing between modules. Using graph theory, the modularity of network organization can be quantified (Meunier et al., 2009b, 2010), where networks with high modularity have dense connections within modules and sparser connections between modules.

Studies examining modular network organization during working memory have shown that increasing executive control demands (i.e., increasing N-back load) are supported by a more integrated network organization, manifested in decreased modularity (Kitzbichler et al., 2011; Vatansever et al., 2015; Wen et al., 2015) and increased connectivity between network modules (Liang et al., 2015; Stanley et al., 2014). This reconfiguration of brain networks has also been observed when comparing networks from a task-free 'resting state' to those during the performance of tasks with increasing demands (Wen et al., 2015).

* Corresponding author at: Helen Wills Neuroscience Institute, University of California, 132 Barker Hall #3190, Berkeley, CA 94720, USA. Tel.: 510 642 2839.
E-mail address: clg5026@berkeley.edu (C.L. Gallen).

In older adults, analyses of structural MRI and resting-state fMRI data have demonstrated that aging is associated with declines in modularity (Chan et al., 2014; Chen et al., 2011b; Geerligs et al., 2014a; Meunier et al., 2009a; Onoda and Yamaguchi, 2013). Importantly, these studies have not examined how networks reconfigure during the performance of a task in older adults. To understand how network-level changes contribute to age-related alterations in executive control, it is critical to investigate changes in brain network properties during cognitive processing.

In this study, we examine how the modular organization of the brain reconfigures between the absence of a task (e.g., a resting state) and the performance of an N-back task in older and young adults. We first quantify the topological overlap of modules identified during resting state and task. We next examine changes in between-module connectivity with increasing cognitive demands, both across the entire brain (i.e., modularity) and in a subset of lateral frontal regions. We also examine how changes in between-module connectivity from a resting state to task are related to behavioral performance. Finally, as aging is associated with declines in white matter pathways (Bennett and Madden, 2014), we investigate how frontal-posterior structural connectivity is related to functional reconfiguration of brain networks in older adults.

2. Material and methods

2.1. Participants

Eighteen young (10 females; mean age = 21.08, range = 18–26) and 38 older (24 females; mean age = 66.97, range = 60–80) adults were included in this analysis. Young and older participants were matched on distribution of gender ($\chi^2(1, N = 56) = 0.30, p = 0.59$). Older participants had greater years of education compared with young participants (mean ± standard error of the mean, older: 17.42 ± 0.49; young: 14.53 ± 0.48; t(54) = 3.67, $p = 0.001$). Participants were prescreened for the presence of medical, neurological, or psychiatric illness (e.g., stroke, traumatic brain injury) and the use of prescribed drugs with known effects on cognition (e.g., benzodiazepines). Older participants were recruited through the Berkeley Aging Cohort and through the community (e.g., fliers, senior residences). Older participants were normal on cognitive screening (i.e., no score less than 1.5 standard deviations below expected performance in more than one cognitive domain for neuropsychological assessments of memory, concentration, verbal fluency, and visuospatial function). A complete neuropsychological evaluation was not available for one subject; however, this subject had a Mini-Mental State Examination score of 28. Young participants were recruited after the collection of older subject data through research study postings at the University of California, Berkeley. Informed consent was obtained from all participants in accordance with the Committee for Protection of Human Subjects at the University of California, Berkeley.

2.2. Cognitive task

The cognitive task performed during fMRI scanning was an N-back task that consisted of 20 runs lasting approximately 2 minutes each (Chen et al., 2011a; Lee and D'Esposito, 2012). Each run contained a series of pseudo-randomly interleaved face and natural scene stimuli (10 of each) during which participants were instructed to either attend to and maintain images from the relevant stimulus category, while ignoring images from the irrelevant category, or to attend both categories. Each stimulus was presented for 600 ms, with a 2.4, 4.4, or 6.4 second jittered delay (randomly ordered) between each stimulus presentation. The 4 conditions varied in executive control demands

and were referred to as: "CATEGORIZE," "SCENES," "FACES," and "BOTH." In CATEGORIZE, participants indicated with a button press whether the current image was a face or a scene, with no attempt to remember the image. In SCENES and FACES, participants were instructed to selectively attend to and maintain images from the relevant category (i.e., scenes or faces, respectively) and ignore images from the irrelevant category (i.e., faces or scenes, respectively). Participants indicated if the current-attended image matched the previous image in the same category. Participants responded to all unattended items in SCENES and FACES with the "no-match" button. Finally, in BOTH, participants were instructed to attend to and maintain both the face and scene stimuli. If the current image matched the previous image of the same category, participants pressed the "match" button. Participants completed 5 blocks of each condition during fMRI scanning.

2.3. MRI acquisition and preprocessing

MRI scans were collected with a 12-channel head coil on a 3T Siemens Trio scanner at the University of California, Berkeley. A high-resolution T1-weighted MP-RAGE sequence was used to acquire 3D anatomical images (repetition time [TR] = 2300 ms, echo time [TE] = 2.98 ms, flip angle = 9°, 1.00-mm^3 voxels). A T2*-weighted echoplanar imaging (EPI) sequence was used to acquire resting state and task functional data (TR = 1000 ms, TE = 27 ms for older participants; 24 ms for young participants, 5.00-mm thick interleaved (descending for young participants) axial slices (0.50-mm gap), in-plane resolution = 3.50 mm^2). Functional data for older adults were collected using GRAPPA with an acceleration factor of 2. For the N-back task scans, five 114-volume runs of each task condition were collected. For the resting state scans, one 300-volume run was collected for all young and 35 older adults. We collected the resting state scans for the remaining 3 older adults with the following parameters: 435 volumes, TR = 1370 ms, TE = 26 ms, 3.50-mm thick interleaved axial slices (0.35-mm gap), in-plane resolution = 2.34 mm^2.

Standard preprocessing of EPI data was carried out with AFNI, versions 2.61–4.21 (Cox, 1996). EPI volumes were slice-time and motion corrected, coregistered to the T1-weighted structural image using a 12-parameter affine transformation, and scaled to have each voxel's run mean be equal to 100. Structural scans were segmented into cerebrospinal fluid and gray and white matter components using SPM8 (Wellcome Department of Cognitive Neurology, London, UK). Functional data were spatially smoothed to a 6-mm full width at half maximum Gaussian kernel and signals (mean and temporal derivative) from white matter, cerebrospinal fluid, and motion were regressed out.

Diffusion-weighted images were acquired for 32 older participants along 30 noncollinear diffusion-encoding directions (50 slices, TR = 6400 ms, TE = 87 ms, field of view: 256 × 256 mm^2, 128 × 128 matrix, 2-mm thick axial slices, in-plane resolution = 2.2 mm^2). The data were preprocessed using the functional magnetic resonance imaging in the brain software library (FSL; Smith et al., 2004; Woolrich et al., 2009). First, the digital imaging and communications in medicine files of each acquisition were converted to a single multivolume 4D format in the MRIcron software (Rorden et al., 2007). Next, they were corrected for any effects of head movement and eddy current distortion using the eddy correct tool in functional magnetic resonance imaging in the brain's diffusion toolbox (FDT). This tool conducts an affine registration of each individual volume to a specified b0 volume. Brain tissue was segmented using the Brain Extraction Tool (Smith, 2002) in FSL, and a brain mask was created at a threshold of 0.3 as recommended by FSL. Diffusion-weighted images were also collected for 16 young adults but not analyzed here.

2.4. Functional connectivity analyses

Participants' T1-weighted anatomical scans were parcellated into 90 cortical and subcortical regions of interest (ROIs) from the automated anatomical labeling (AAL) atlas (Tzourio-Mazoyer et al., 2002). ROIs were reverse-normalized to each participant's native space using the parameters from SPM segmentation (i.e., a reverse normalization from the warping to Montreal Neurological Institute (MNI) template space that was computed during segmentation). Individual time-series from each resting state and task run were averaged over the voxels in each ROI and bandpass filtered (0.009–0.08 Hz) to remove physiological artifacts. Six ROIs were excluded from subsequent analyses because they were missing coverage in the EPI volumes in some scanning runs in either young or older participants (bilateral inferior occipital gyrus, left fusiform gyrus, right superior parietal gyrus, left middle temporal pole, left inferior temporal gyrus). Finally, functional connectivity matrices for resting state and task were created for each participant by correlating the time-series between each pair of ROIs using Pearson's correlation coefficient and applying a Fisher z-transform. As there are multiple methods for parcellating the brain into ROIs for network analyses, we also repeated our analyses with a commonly used atlas that is composed of functionally, rather than anatomically, defined regions from healthy young subjects (Power et al., 2011).

We matched whether resting state scans were acquired before or after the N-back task in the young and older groups. Resting-state scans were collected after the task for 26 older and 13 young adults; the remaining participants had resting-state scans collected before the task (12 older and 5 young). The distribution of pre-task and post-task resting-state scans across participants was equivalent between the 2 age groups (χ^2(1, N = 56) = 0.08, $p = 0.77$). Additional follow-up analyses in Section 3.4 address the potential effects of pre-task and post-task resting-state scans on our results.

To have similar numbers of volumes for resting state and task correlation analyses, 5.7 minutes (342 volumes) of each task condition were analyzed, by demeaning and concatenating 3 of the 5 blocks for each condition before computing correlations between each ROI pair. Concatenating task volumes allows for additional task data to be used to more reliably estimate functional connectivity between ROIs. Furthermore, it makes the amount of data for correlation analyses similar between resting state and task conditions. For 11 young and 29 older adults, we used the first 3 runs of each task condition to generate the task time-series. In a portion of the first 3 runs for the remaining 9 older adults, there were suspected artifacts from movement during the GRAPPA reference scan (autocalibrating signal scan); we therefore used 1 or 2 of the subsequent runs to generate task time-series (12 total time-series across participants and task conditions). We matched the composition of the task time-series for these older participants in a set of 7 young adults. Furthermore, the distribution of whether task time-series were generated from the first 3 runs was matched between the age groups (χ^2(1, N = 56) = 1.38, $p = 0.24$). Additional follow-up analyses in Section 3.4 address the potential effects of task-run selection on our results.

2.5. Module-based network metrics

The functional connectivity matrices were binarized to create adjacency matrices that indicate the presence or absence of a connection between a pair of regions. Matrices were binarized over a range of connection density thresholds, where thresholding of the matrices was achieved by matching the number of network connections across participants (here, the top 5%–25% of all possible connections in the network in 5% increments). Each of these thresholded matrices was used to create unweighted, undirected whole-brain graphs (defined as a set of nodes or ROIs and the edges or connections between them) with which network metrics were examined. Unless otherwise noted, network metrics were created separately for each connection threshold and are presented as the average across all 5 connection density thresholds.

Each brain graph was then subdivided into modules using a simulated annealing algorithm (Kirkpatrick et al., 1983). We subsequently refer to the collection of modules as a "partition." For each graph, we identified its "optimal" modular organization by choosing the partition with the highest modularity value across the algorithm iterations (Newman and Girvan, 2004). Highly modular graphs have dense connections within modules and sparser connections between modules. We then investigated the reconfiguration of modular network structure between a resting state and task in the 2 age groups.

First, as our module-detection procedure allows for different partitions (groupings of nodes into modules) across individuals and task conditions, we investigated the overlap of modules between a resting state and task using mutual information (MI). MI quantifies the similarity of 2 partitions (Danon et al., 2005) with 1 representing identical partitions, and low values indicating that nodes tend to group together into different modules. We compared each subject's resting-state network organization to those created from the 4 task conditions to examine the differences in modules between a resting state and task.

Next, we investigated changes in network connections between resting state and task. We first quantified modularity, a whole-brain network measure that compares the number of connections within to the number of connections between modules (Newman and Girvan, 2004). Modularity will be 1 if all connections fall within modules, and it will be 0 if there are no more connections within modules than would be expected by chance.

Although modularity quantifies the balance of within- and between-module connections across the whole-brain network, there may also be changes in particular network connections in the brain. Thus, we also examined the properties of specific between-module connections that provide communication across network modules. To do so, we quantified the participation coefficient (PC) of individual brain regions, a measure of the distribution of a node's connections across modules (Guimera and Amaral, 2005; Guimera et al., 2006). A node's PC will be 1 if its connections are uniformly distributed across all network modules and it will be 0 if its connections are concentrated within its own module. In other words, a higher PC value suggests that a node's connections are more distributed among network modules, whereas a lower PC value indicates that a node's connections are more concentrated in its own module. We focused on examining PC of lateral frontal regions, as they play a critical role in top-down modulation of sensory cortices (Gazzaley and Nobre, 2012) to support executive control functions such as attention and working memory (Chao and Knight, 1998; Funahashi et al., 1993a, 1993b; Lee and D'Esposito, 2012). Furthermore, older adults exhibit notable impairments in these functions (Clapp et al., 2011; Gazzaley et al., 2005). We calculated PC for 10 lateral frontal regions in the AAL atlas: bilateral precentral, middle frontal, superior frontal, and pars opercularis and pars triangularis of the inferior frontal gyrus. PC was averaged across lateral frontal regions to examine general changes that occur in lateral frontal cortex with aging. To examine the specificity of lateral frontal changes, we also examined PC for 10 control regions in the occipital cortex: bilateral superior occipital, middle occipital, cuneus, calcarine, and lingual gyrus. We restricted our analyses to one set of control regions to limit the number of statistical tests conducted.

2.6. White matter connectivity analyses

We were also interested in investigating the relationship between functional network changes and connectivity of long-range white matter association fiber tracts. We focused on the superior longitudinal fasciculus (SLF), as it has been shown to provide critical anatomical connections between frontal and posterior cortical regions (Makris et al., 2005), putative targets of frontal regions implicated in executive control (Mori et al., 2008). After preprocessing, the FDT tool in FSL was used to fit a diffusion tensor model at each voxel in the brain-extracted images created with Brain Extraction Tool. Fractional anisotropy (FA) maps were derived for each participant. Voxel-wise statistical analysis of the FA data was carried out using tract-based spatial statistics (Smith et al., 2006) in FSL. ROI masks for the left and right SLF were created using the JHU-ICBM-DTI-81 Atlas. These masks were then used to extract the average FA value for the tract across hemispheres in each participant, which we speculate reflects variability in underlying structural connectivity or white matter architecture across participants.

2.7. Statistical analysis

Effects of aging on task performance (i.e., accuracy and reaction time) were assessed with a repeated-measures ANOVA with a within-subjects factor of task condition (CATEGORIZE, SCENES, FACES, BOTH) and a between-subjects factor of age group (OLDER, YOUNG). MI between a resting state and the 4 task network partitions was assessed with a repeated-measures ANOVA with a within-subjects factor of task condition (CATEGORIZE, SCENES, FACES, BOTH) and a between-subjects factor of age group (OLDER, YOUNG). Modularity and PC were assessed with repeated-measures ANOVAs with a within-subjects factor of task condition (RESTING-STATE, CATEGORIZE, SCENES, FACES, BOTH) and a between-subjects factor of age group (OLDER, YOUNG). For ANOVAs that only include the 4 task conditions as factors (i.e., do not include resting state), we report both the overall within-subjects effects of task condition and the linear within-subjects contrasts, as we hypothesized that the task conditions would modulate outcome measures in a parametric fashion. We present descriptive statistics (mean and standard deviation) for these measures in Table 1.

We set a significance threshold of $p < 0.05$ and also report nonsignificant trends at $p < 0.10$. To ensure maximal transparency, we report uncorrected p-values and interpret results with caution when they do not pass a Bonferroni-corrected threshold for 3 tests (MI, modularity, and lateral frontal PC). For all ANOVAs, we also report estimates of effect size for each contrast as partial eta-squared (η_p^2). Significant interactions between age group and task condition were subsequently investigated with post hoc comparisons, focusing on age group differences across resting state and task conditions.

Recent work has shown that in-scanner motion can spuriously affect measures of functional connectivity (Power et al., 2012, 2013; Satterthwaite et al., 2013; Van Dijk et al., 2012). We took several steps to ensure that the reconfiguration of modular network structure was not related to motion. First, we examined age and task differences in head motion, quantified as the Euclidean norm of the derivatives of motion parameters. Second, we conducted all network analyses with motion as a covariate of no interest.

Finally, we examined behavioral and structural correlates of network reconfiguration in older adults. We quantified network reconfiguration as the change in lateral frontal PC between resting state and task (averaged across all task conditions). Correlations were quantified with Spearman's rho instead of Pearson's correlation coefficient to reduce the influence of extreme values. To examine the relationship between network reconfiguration and

Table 1
Mean (SD) of task performance and network metrics (AAL atlas) for young and older adults

	Resting state		Categorize		Scenes		Faces		Both	
	Young	Older	Young	Older	Young	Older	Young	Older	Young	Older
Accuracy (%)	N/A	N/A	95.83 (5.25)	95.35 (9.92)	96.39 (5.12)	92.98 (7.66)	94.91 (3.68)	87.11 (10.88)	91.94 (6.94)	83.55 (9.05)
RT (ms)	N/A	N/A	629.33 (113.74)	647.47 (150.86)	671.40 (144.62)	753.98 (159.79)	745.98 (163.99)	838.63 (154.67)	837.89 (168.70)	1020.22 (187.76)
MI	N/A	N/A	0.31 (0.06)	0.21 (0.08)	0.32 (0.09)	0.21 (0.08)	0.31 (0.09)	0.18 (0.07)	0.29 (0.07)	0.19 (0.07)
Mod	0.43 (0.04)	0.36 (0.07)	0.41 (0.06)	0.35 (0.06)	0.42 (0.07)	0.34 (0.05)	0.43 (0.04)	0.33 (0.06)	0.39 (0.04)	0.33 (0.06)
Frontal PC	0.28 (0.09)	0.29 (0.09)	0.25 (0.08)	0.35 (0.06)	0.24 (0.08)	0.34 (0.08)	0.29 (0.09)	0.35 (0.09)	0.31 (0.05)	0.34 (0.07)
Occipital PC	0.23 (0.08)	0.24 (0.11)	0.25 (0.09)	0.28 (0.08)	0.29 (0.11)	0.28 (0.11)	0.26 (0.08)	0.30 (0.11)	0.27 (0.10)	0.29 (0.08)

Key: AAL, automated anatomical labeling; MI, mutual information; Mod, Modularity; PC, participation coefficient; RT, reaction time; SD, standard deviation.

executive control, we conducted correlations between the change in lateral frontal PC and behavioral performance (reaction time) from the task. Differences in correlation values between older and young groups were evaluated using the formula described by Cohen (Cohen et al., 2003) after using the conversion from Spearman's to Pearson's coefficients described by Myers and Sirois (Myers and Sirois, 2004). To examine the relationship between white matter architecture and network reconfiguration in older adults, we conducted correlations between FA of the SLF (average of left and right hemispheres) and the change in lateral frontal PC.

Plots were created with the Matplotlib package (http://matplotlib.org/) in IPython (http://ipython.org/) and brain network graphs were visualized with BrainNet Viewer (http://www.nitrc.org/projects/bnv/).

3. Results

3.1. Task performance

Accuracy and reaction time (RT) analyses revealed main effects of age group (accuracy: $F(1,54) = 5.74$, $p = 0.02$, $\eta_P^2 = 0.10$; RT: $F(1,54) = 5.03$, $p = 0.03$, $\eta_P^2 = 0.09$) and task condition (accuracy: overall effect, $F(3,162) = 28.50$, $p < 0.001$, $\eta_P^2 = 0.35$ and linear contrast, $F(1,54) = 60.04$, $p < 0.001$, $\eta_P^2 = 0.53$; RT: overall effect, $F(3,162) = 141.90$, $p < 0.001$, $\eta_P^2 = 0.72$ and linear contrast, $F(1,54) = 200.92$, $p < 0.001$, $\eta_P^2 = 0.79$). Across all conditions, older adults had lower accuracy and longer RTs than young adults. Across all participants, accuracy was highest and RTs were shortest in the CATEGORIZE and SCENES conditions, followed by FACES and BOTH.

The age group by task condition interaction was also significant for both accuracy and RT (accuracy: $F(3,162) = 7.75$, $p < 0.001$, $\eta_P^2 = 0.13$; RT: $F(3,162) = 10.47$, $p < 0.001$, $\eta_P^2 = 0.16$), indicating that older adults performed worse than young adults but not equally in all conditions. Older and young adults had equivalent accuracy and RT in the CATEGORIZE condition (accuracy: $p = 0.85$; RT: $p = 0.65$), but older adults had lower accuracy (Fig. 1A) and longer RTs (Fig. 1B) than young adults in the SCENES, FACES, and BOTH conditions (accuracy: $p = 0.09$, $p = 0.005$, $p = 0.001$; RT: $p = 0.07$, $p = 0.05$, $p = 0.001$). We also conducted nonparametric tests (Mann-Whitney U test) between the age groups for each task condition. These results confirmed that older adults performed less accurately and slower on all conditions except for CATEGORIZE (accuracy: CATEGORIZE, $p = 0.85$; SCENES, $p = 0.02$; FACES, $p < 0.001$; BOTH, $p < 0.001$; RT: CATEGORIZE, $p = 0.66$; SCENES, $p = 0.03$; FACES, $p = 0.04$; BOTH, $p = 0.001$).

3.2. Reconfiguration of modular network organization during executive control processing

3.2.1. Mutual information between network partitions during resting state and task performance

We first examined changes in modules between resting state and task in young and older adults. More specifically, we quantified the MI between each subject's resting network partition and those derived from the 4 task conditions, thus producing 4 MI values (each task condition compared with resting state) for each subject. A repeated-measures ANOVA on MI revealed main effects of age group and task condition (Fig. 2A; age group: $F(1,54) = 33.22$, $p < 0.001$, $\eta_P^2 = 0.38$; task condition: overall effect, $F(3,162) = 2.11$, $p = 0.10$, $\eta_P^2 = 0.04$ and linear contrast, $F(1,54) = 4.33$, $p = 0.04$, $\eta_P^2 = 0.07$). Across all task conditions, older adults had lower MI between resting state and task than young adults. The significant linear contrast suggests that MI was modulated parametrically across the task conditions. Across all participants, MI between resting state and task was higher for CATEGORIZE and SCENES
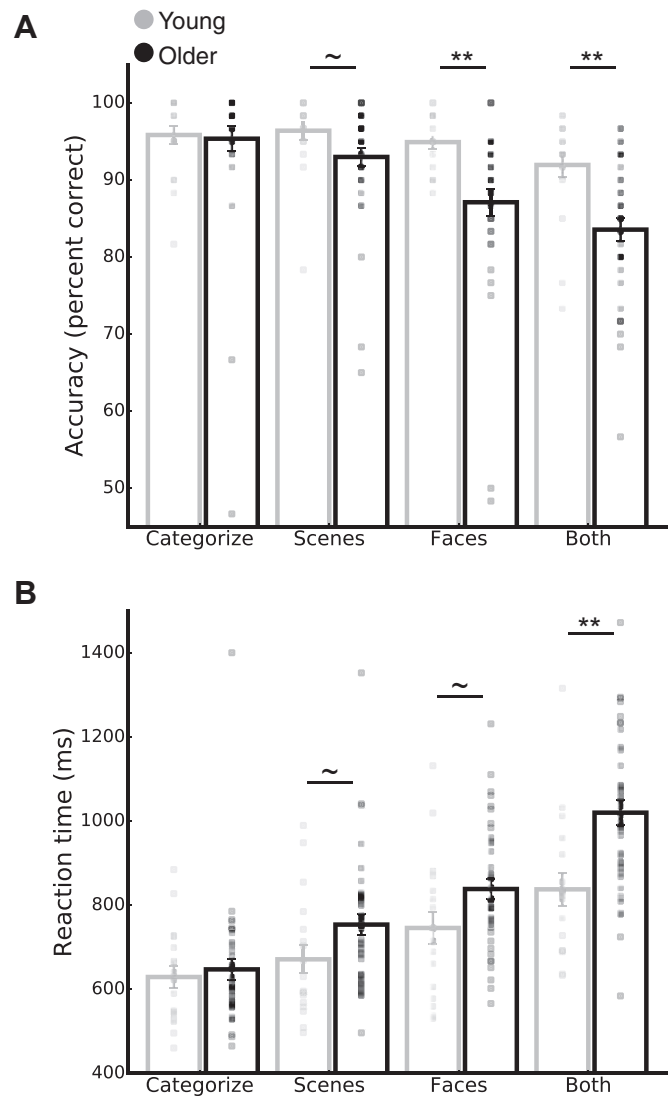

Fig. 1. Task accuracy (A) and reaction time (B) for young and older adults. Data are presented as mean ± standard error of the mean. Pairwise comparisons between young and older groups across the task conditions were conducted for metrics showing significant age group by task condition interactions. $^{**}p < 0.01$; $^{\sim}p < 0.1$.

compared with BOTH and higher in SCENES compared with FACES. The main effect of task condition on MI should be interpreted with caution, as it does not pass a Bonferroni-corrected significance threshold of $p < 0.05$. There was no significant age group by task condition interaction ($F(3,162) = 0.56$, $p = 0.64$, $\eta_P^2 = 0.01$).

3.2.2. Modularity of the brain during resting state and task performance

We next examined changes in the balance of within- and between-module connections across the whole brain by quantifying the modularity of the network. ANOVAs on modularity revealed a main effect of age group ($F(1,54) = 43.38$, $p < 0.001$, $\eta_P^2 = 0.45$) and task condition ($F(4,216) = 2.59$, $p = 0.04$, $\eta_P^2 = 0.05$). Across all task conditions, older adults had lower modularity than young adults. Across all participants, RESTING-STATE, CATEGORIZE, SCENES, and FACES conditions were associated with higher modularity than the BOTH condition (Fig. 2B). Although the main effect of task condition on modularity using the AAL atlas does not pass a Bonferroni-corrected significance threshold of $p < 0.05$, we
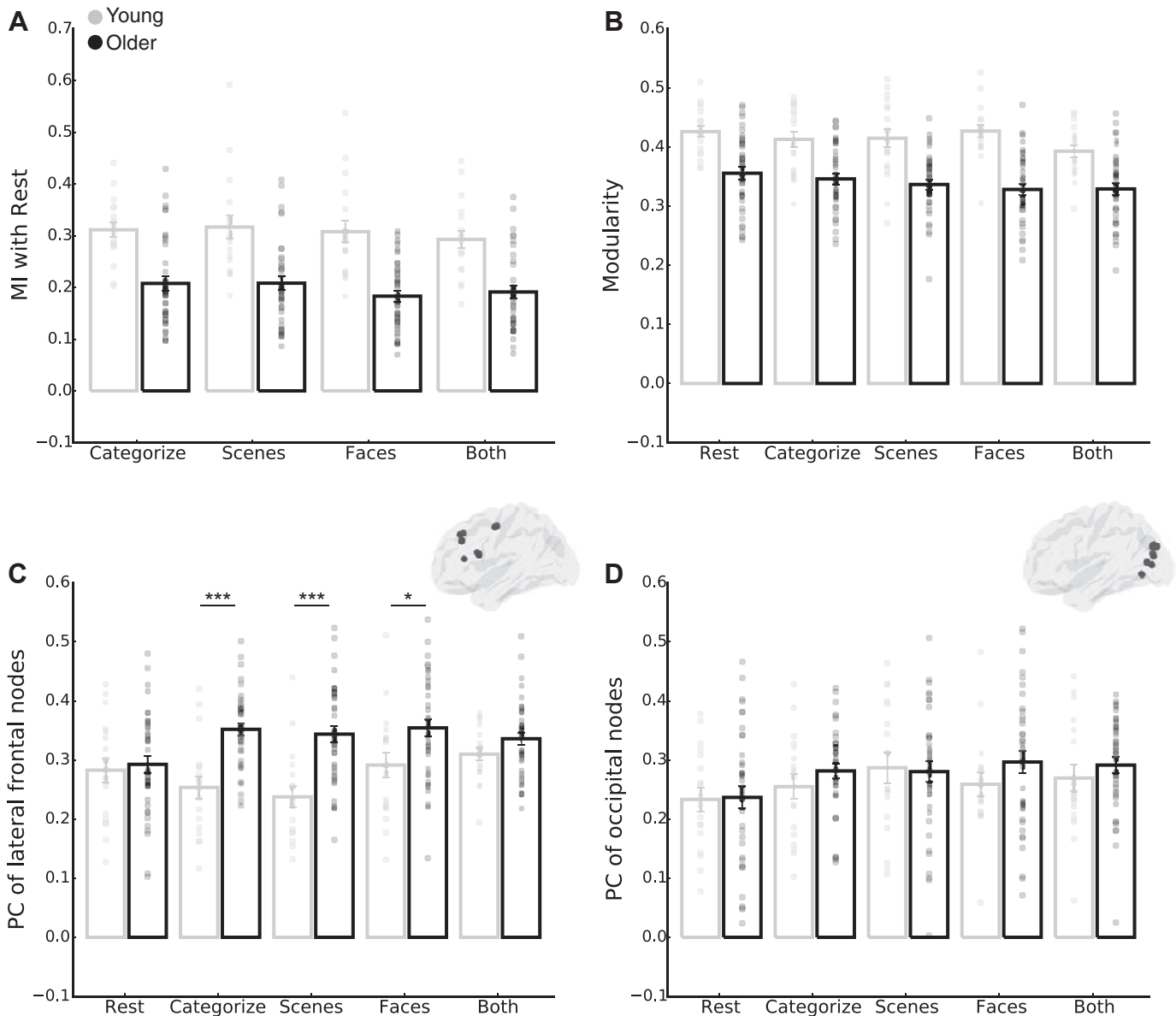
Fig. 2. Module-based network metrics during resting state and task. (A) Mutual information (MI) between resting state network partitions and those derived from the task conditions. Note that we quantified the MI between each subject's resting network partition to those derived from the 4 task conditions. In this manner, MI during resting state would be equal to 1 because it is the network used for comparison and is therefore not plotted in (A). Modularity (B) and lateral frontal (C) and occipital (D) participation coefficient (PC) for resting state and task conditions. Centers of mass for lateral frontal and occipital AAL atlas nodes used to calculate PC are plotted on a sagittal view of the brain in C and D, respectively. Data are presented as mean ± standard error of the mean. Pairwise comparisons between young and older groups across the task conditions were conducted for metrics showing significant age group by task condition interactions. ***$p < 0.001$; *$p < 0.05$.

replicated this result using the Power et al. (2011) atlas (main effect of task condition, corrected $p < 0.05$; see Supplementary Material). There was no significant age group by task condition interaction ($F(4,216) = 1.12$, $p = 0.35$, $\eta_P^2 = 0.02$).

3.2.3. Participation coefficient of lateral frontal regions during resting state and task performance

To examine the specific contribution of lateral frontal connections to network reconfiguration, we quantified the distribution of between-module connections (i.e., PC) from 10 lateral frontal regions in the AAL atlas (Fig. 2C). An ANOVA on lateral frontal PC revealed main effects of age group ($F(1,54) = 18.26$, $p < 0.001$, $\eta_P^2 = 0.25$) and task condition ($F(4,216) = 2.96$, $p = 0.02$, $\eta_P^2 = 0.05$). Across all task conditions, older adults had higher frontal PC than young adults. Across all participants,

frontal PC was lower during RESTING-STATE and SCENES compared with FACES and BOTH. The main effect of task condition on lateral frontal PC passes a marginal Bonferroni-corrected significance threshold of $p < 0.1$.

There was also a significant age group by task condition interaction ($F(4,216) = 4.68$, $p = 0.001$, $\eta_P^2 = 0.08$), indicating that the increased frontal PC in older adults was not equivalent across all task conditions (Fig. 3). Specifically, although there were no differences in lateral frontal PC between older and young adults during a resting-state condition ($p = 0.70$), older adults showed increased frontal PC compared with young adults during the 3 less-demanding task conditions (CATEGORIZE, $p < 0.001$; SCENES, $p < 0.001$; FACES, $p = 0.02$). Furthermore, there were no significant differences between older and young adults in the BOTH condition ($p = 0.14$). This suggests that older adults exhibited a task-related
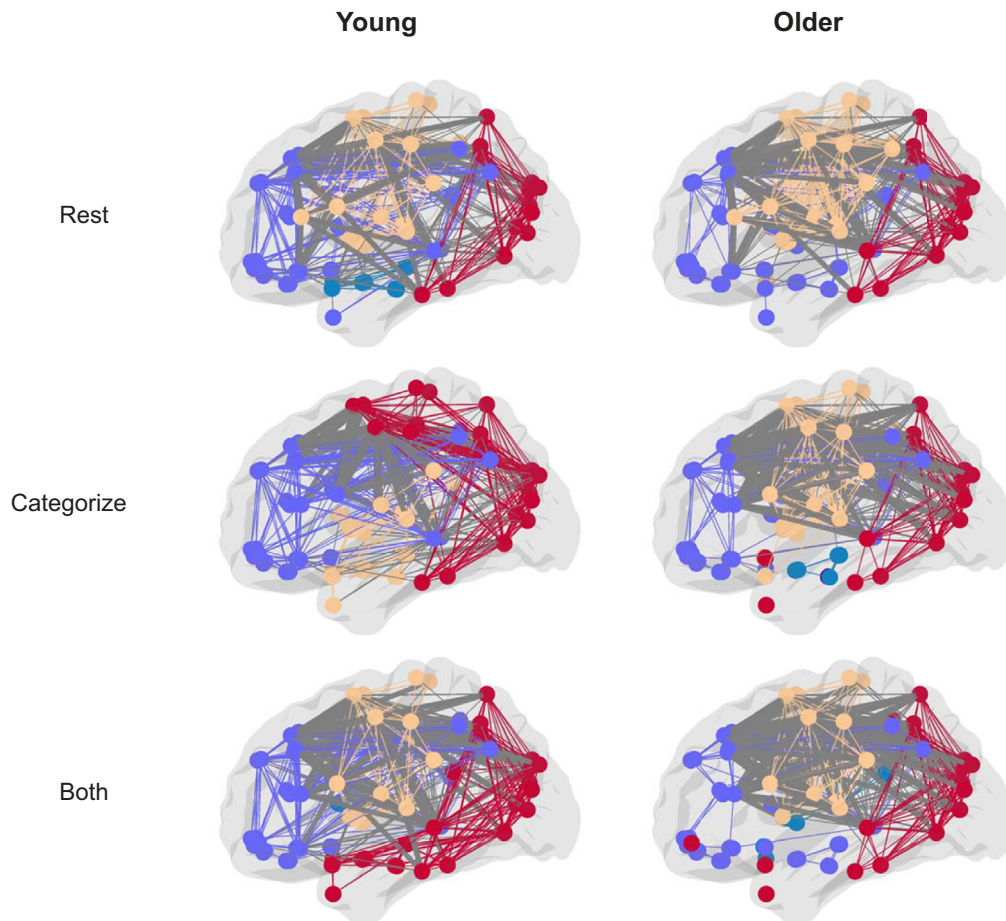
Young **Older**

Rest

Categorize

Both

Fig. 3. Sagittal views of group partitions during resting state (top) and the least and most demanding task conditions (middle and bottom, respectively) for young and older adults. For visualization purposes, group consensus partitions were created by averaging the AAL atlas correlation matrices across subjects in each group and thresholding at 20% of possible network connections (although note that all analyses presented in the results were done at the individual subject level at multiple connection thresholds as described in the methods). Within-module edges are colored to match that of nodes in their own module and between-module edges are colored gray, with lateral frontal between-module connections bolded. Older adults show more between-module lateral frontal connections at lower levels of demand (CATEGORIZE) compared with young adults. Young and older adults have similar amounts of lateral frontal connections during resting state and the more demanding task condition (BOTH).

increase in lateral frontal PC during all conditions, whereas young adults only exhibited an increase during the most demanding condition. Importantly, this age group by task condition interaction was not present in 10 control regions from the occipital cortex (Fig. 2D; F(4,216) = 0.55, $p = 0.70$, $\eta_P^2 = 0.01$), suggesting that the age-related reconfiguration of between-module connections may be specific to the lateral frontal cortex.

3.2.4. Behavioral correlates of network reconfiguration in older adults

To investigate how changes in between-module connections in lateral frontal cortex during task performance are related to individual differences in behavior, we correlated task-based reconfiguration of lateral frontal PC (i.e., difference between task and resting state) and mean task RT. We averaged PC for each task condition, given that older adults exhibited increases in PC across all task conditions. Older adults who exhibited greater task-based increases in lateral frontal PC had faster task performance (Fig. 4A; rho(36) = −0.32, $p = 0.05$), whereas this relationship was not present in young adults (rho(16) = 0.31, $p = 0.21$). The difference in correlations between older and young groups was statistically significant ($p = 0.03$). Critically, the correlation in older adults was only present when quantifying the difference in lateral frontal PC between resting state and task; there was no correlation

between task performance and lateral frontal PC during resting state or task alone in older adults (RESTING-STATE, $p = 0.14$; TASK, $p = 0.76$).

3.2.5. Replication analyses of changes in network reconfiguration

We reproduced the results of this study using a different brain parcellation scheme comprised of functionally defined ROIs (Power et al., 2011), with 2 separate approaches. First, we used spectral clustering to identify network modules for each subject and task condition. Although simulated annealing is one of the most accurate methods to identify modules (Guimera and Amaral, 2005), it is computationally intensive. Thus, for this larger set of ROIs, we identified modules using a spectral clustering algorithm (Newman, 2006) that provides a tradeoff between accuracy and expediency, after thresholding the correlation matrices similar to previous reports (Power et al., 2011): the top 2%−10% of connections in 5% increments. This is an approach we have taken previously (Sadaghiani et al., 2015). Second, we used predefined modules previously identified in a group of individuals (Power et al., 2011), thus applying the same modular partition across all individuals rather than identifying modules with a clustering algorithm. This approach allowed us to examine changes in the connections between modules that are not influenced by changes in the grouping of nodes into modules themselves. In other words, the modules were fixed for
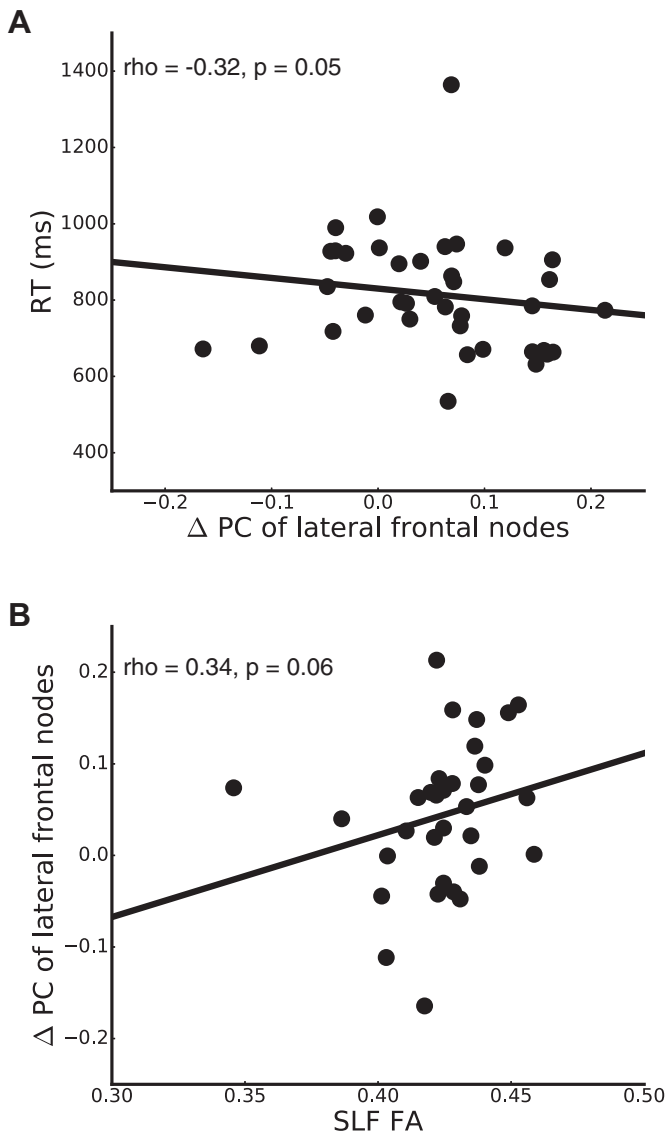
A

B

Fig. 4. Relationship between change in lateral frontal PC from resting state to task and executive control task performance (RT; A) and fractional anisotropy (FA) of the superior longitudinal fasciculus (SLF; B) in older adults. Abbreviations: PC, participation coefficient; RT, reaction time.

all subjects, and we then examined changes in the connectivity between modules (i.e., modularity and lateral frontal PC). Using these 2 approaches, we reproduced our previous results for changes in module-based network metrics and correlations with task performance (see Supplementary Material).

3.3. Structural correlates of network reconfiguration in older adults

To investigate how the age-related functional reconfiguration of between-module connections in lateral frontal cortex is related to structural connectivity, we correlated task-based reconfiguration of lateral frontal PC and FA of the SLF in older adults (mean ± standard deviation, 0.42 ± 0.02). Older adults who exhibited greater task-based increases in lateral frontal PC had marginally greater FA of the SLF (Fig. 4B; rho(30) = 0.34, $p = 0.06$). Although the correlation with 10 lateral frontal ROIs from the AAL atlas was marginally significant, we replicated this result using 30 lateral frontal ROIs from the Power et al. (2011) atlas when modules were identified

with spectral clustering. Using this atlas, greater task-based increases in lateral frontal PC were significantly related to greater SLF FA ($p = 0.02$; see Supplementary Material).

3.4. Consideration of confounds on network reconfiguration in older adults

We first examined the effects of head motion on measurements of network organization. Although head motion was higher in older adults across all task conditions (F(1,54) = 13.37, $p = 0.001$), there was no effect of task condition or age group by task condition interaction on motion (F(4,216) = 0.22, $p = 0.83$; F(4,216) = 0.80, $p = 0.46$). Importantly, head motion did not differ between resting state and task in either the older or young groups ($p = 0.91$; $p = 0.98$), suggesting that the age differences in network reconfiguration between resting state and task were not driven by differences in head motion between conditions in the age groups. Furthermore, including head motion as a covariate in the AAL network analyses did not substantially change any results.

We also examined effects of the time period of resting data collection on measurements of network organization. Although the proportion of resting-state scans before or after the task was matched in the older and young groups, it is possible that there were group differences (i.e., an age group by resting-state position interaction). To test this, we repeated all AAL network analyses with resting-state position (i.e., before or after the task) as an additional between-subjects factor. There was no significant 2-way interaction between age group and resting-state position or 3-way interaction between age group, resting-state position, and task condition for MI, modularity, or lateral frontal PC. This suggests that the effects reported are not differentially present whether the resting-state scan was collected before or after the task.

Finally, we examined the effect of task-run selection on measurements of network organization. We repeated all AAL network analyses with task position (i.e., first 3 runs or containing some subsequent runs) as an additional between-subjects factor. There was no significant 2-way interaction between age group and task position or 3-way interaction between age group, task position, and task condition for MI, modularity, or lateral frontal PC. These results suggest that the results reported are not differentially present whether the task time-series were composed of the first 3 runs or subsequent runs.

4. Discussion

Here, we analyzed resting state and task-based fMRI data to characterize brain network reconfiguration that supports executive control functioning (i.e., performance of an N-back task) in older adults. Recent studies have shown that older adults have a less-modular brain network organization in a resting state compared with young adults (Chan et al., 2014; Geerligs et al., 2014a; Onoda and Yamaguchi, 2013). However, the extent to which this organization reconfigures during a cognitive task in older adults remains underspecified. We provide evidence that older adults exhibit larger changes in network organization at lower levels of N-back task demands compared with young adults. More specifically, older adults showed greater between-module connectivity of lateral frontal regions compared with young adults at low levels of executive control demands. In older adults, greater network reconfiguration (i.e., increased between-module connections of lateral frontal regions) from resting state to task was related to better task performance, suggesting that greater between-module integration during task performance is critical for successful executive control

in aging. Finally, network reconfiguration from resting state to task in older adults was related to individual variability in white matter microstructure of the SLF, the main tract connecting frontal and posterior brain regions.

4.1. Changes in topological overlap of modules between resting state and task

We found that older adults had less overlap between modules present during a task-free resting state and those present during the performance of an N-back task. In other words, the composition of modules identified during a resting state changed more during the task in older adults compared with young adults. This finding suggests that older adults exhibited greater reconfiguration of network modules detected during a resting state while performing a task.

Furthermore, across both young and older adults, we found that modules identified during the more challenging task conditions had less overlap with resting-state modules, suggesting that resting modular organization changed more during higher task demands. This latter finding is consistent with a previous study in young participants showing that there was less overlap of modules across subjects (e.g., more variability in the modules across subjects) during a more difficult N-back condition (Stanley et al., 2014). This result and ours adds to a growing literature suggesting that the modular organization of the brain shows more pronounced reconfigurations with increasing cognitive demands.

4.2. Reconfiguration of modular brain network organization during resting state and task

We found that older adults exhibited lower modularity than young adults during a resting state, which supports accumulating evidence that aging reduces the segregation of networks into distinct modules when measured in the absence of a task (Chan et al., 2014; Geerligs et al., 2014a; Onoda and Yamaguchi, 2013). Decreased modularity in older adults has been hypothesized to reflect reduced functional integrity of brain network modules, in which brain subnetworks are less segregated in older adults compared with young adults. We further found that older adults had lower modularity than young adults during the N-back task, suggesting that such global age differences in brain network organization are also present throughout task performance.

In addition, across both young and older adults, we found that modularity decreased with increasing task demands. This is consistent with previous findings in young adults examining network changes during task performance. First, prior work has shown that within-module connections decrease and between-module connections increase from resting state to task (Cole et al., 2014). Second, studies have shown that modularity decreases with increasing working memory load and that this reconfiguration is related to better task performance (Kitzbichler et al., 2011; Stanley et al., 2014; Vatansever et al., 2015). We found a similar pattern of results, in which the most demanding conditions of the N-back task were associated with the lowest modularity and extend this work by showing similar effects across both young and older adults. Changes in modularity due to increasing cognitive demands are proposed to reflect increased integration between brain network modules to support higher processing demands. Furthermore, it has been proposed that reductions in modularity with increasing cognitive effort represent the formation of a neuronal "workspace" (Dehaene et al., 1998) that supports more efficient communication across the brain (Kitzbichler et al., 2011).

4.3. Alterations in between-module connections with increasing task demands

Although we found that modularity was reduced in older adults during a resting state and task performance, we also examined how specific between-module connections reconfigured during these conditions in young and older adults. We found that young and older adults had similar between-module connectivity (PC) of lateral frontal regions during a resting state, and that older adults exhibited increased connectivity during all task conditions. Specifically, older adults had greater between-module connectivity than young adults during the less-demanding conditions, but similar between-module connectivity in the most demanding condition (i.e., BOTH). These results suggest that older adults recruited additional between-module connections at all levels of task demand, whereas young adults only did so when task demands were highest. Furthermore, in older adults, greater network reconfiguration from a resting state to task was associated with better task performance. Not surprisingly, this relationship was not present in young adults, given that they did not show an increase in lateral frontal PC for most of the task conditions. Finally, we found that greater network reconfiguration from a resting state to task in older adults was associated with greater FA of the SLF, a core frontal-posterior white matter tract. Our results support the "workspace" hypothesis: increased cognitive effort is associated with increased between-module integration that is related to better task performance (Kitzbichler et al., 2011; Stanley et al., 2014; Vatansever et al., 2015). Here, we provide new evidence that older adults exhibit increased between-module integration at lower levels of cognitive demand than young adults. It should be noted that older adults showed this reconfiguration even when performance was equivalent to young adults in terms of accuracy and reaction time (e.g., during CATEGORIZE), suggesting that network changes were not merely due to the differences in performance between the older and young groups.

Most studies examining age-related changes in brain function due to specific cognitive demands have examined the activation of individual brain regions, rather than using a large-scale network approach. In particular, numerous studies have shown that older adults exhibit increased frontal activity during less-demanding cognitive tasks compared with young adults (Mattay et al., 2006; Spreng et al., 2010; Turner and Spreng, 2012, 2015). Together, these studies have been interpreted to reflect the recruitment of additional neural resources that support cognition at lower levels of cognitive demand (Reuter-Lorenz and Cappell, 2008). Our results further support the idea of compensatory recruitment and, importantly, suggest a large-scale network-level mechanism by which the aging brain reorganizes to support executive control processing. Although our correlation analyses cannot provide information about directionality, we propose that greater structural connectivity of frontal-posterior white matter pathways enables older adults to appropriately reconfigure brain networks between a resting state and task performance, depending on the task demands. Specifically, older adults showed greater increases in lateral frontal between-module connections at lower levels of demand compared with young adults. We postulate that this pattern of increased connectivity between frontal regions and other modules is reflective of a more integrated network architecture that is important for successful executive control processing in aging.

Future work should investigate how other changes that occur with aging (e.g., reductions in cerebral gray matter) are related to functional network reconfiguration. Furthermore, as aging is associated with cognitive changes in other domains, such as long-term memory, an important future step would be to quantify network changes during other cognitive tasks. There is some

evidence that older adults show larger connectivity changes in nonfrontal regions (i.e., parietal and somatosensory cortex) with increasing task demands compared with young adults (Geerligs et al., 2014b). The network reconfiguration reported here could be a domain-general response to increasing cognitive demands or there could be unique changes for the processing of specific cognitive functions.

4.4. Methodological considerations

There are many valid approaches to examine brain network properties with fMRI data. Regarding methods for parcellating the brain into ROIs, we demonstrated that our results are reproducible for both anatomically (Tzourio-Mazoyer et al., 2002) and functionally (Power et al., 2011) defined ROIs. Although the larger ROIs in the AAL atlas may encompass multiple functional regions, there may also be drawbacks to using a functionally defined atlas when comparing groups of young and older adults. Specifically, most functionally defined atlases have been created using data from young subjects. Thus, differences in functional boundaries in older adults could bias network measures in a way that an anatomically defined atlas would not. Given this, the replication of our results using an anatomical and functional atlas demonstrates the robustness of our findings. Future work should examine how potential changes in the functional boundaries of brain regions in older adults influence network measures.

Regarding methods for identifying brain network modules, subject-level modular networks may be noisier than those derived at the group level (e.g., identifying modules after averaging correlation matrices across subjects). Furthermore, if the modules are different across subjects, changes in network connections could arise from differences in the modules themselves and/or changes in connectivity. Although we examined the overlap in modules with MI, we also replicated our results after imposing the same modular organization across all subjects.

Finally, although our primary findings demonstrated an interaction between age group and task condition, we reported several main effects of age group on network organization (e.g., MI and modularity). We cannot rule out the possibility that these effects are due to age-related changes in vasculature that may impact the BOLD signal, anatomical changes in gray and white matter (D'Esposito et al., 2003), or differences in functional image acquisition between older and young adults.

Disclosure statement

The authors declare no competing financial interests.

Acknowledgements

Appendix A. Supplementary data

Supplementary data associated with this article can be found, in the online version, at http://dx.doi.org/10.1016/j.neurobiolaging.2016.04.003.

References

Andrews-Hanna, J.R., Snyder, A.Z., Vincent, J.L., Lustig, C., Head, D., Raichle, M.E., Buckner, R.L., 2007. Disruption of large-scale brain systems in advanced aging. Neuron 56, 924–935.

Barceló, F., Suwazono, S., Knight, R.T., 2000. Prefrontal modulation of visual processing in humans. Nat. Neurosci. 3, 399–403.

Bennett, I.J., Madden, D.J., 2014. Disconnected aging: cerebral white matter integrity and age-related differences in cognition. Neuroscience 276, 187–205.

Chan, M.Y., Park, D.C., Savalia, N.K., Petersen, S.E., Wig, G.S., 2014. Decreased segregation of brain systems across the healthy adult lifespan. Proc. Natl. Acad. Sci. U. S. A. 111, E4997–E5006.

Chao, L.L., Knight, R.T., 1998. Contribution of human prefrontal cortex to delay performance. J. Cogn. Neurosci. 10, 167–177.

Chen, A.J.W., Novakovic-Agopian, T., Nycum, T.J., Song, S., Turner, G.R., Hills, N.K., Rome, S., Abrams, G.M., D'Esposito, M., 2011a. Training of goal-directed attention regulation enhances control over neural processing for individuals with brain injury. Brain 134, 1541–1554.

Chen, Z.J., He, Y., Rosa-Neto, P., Gong, G., Evans, A.C., 2011b. Age-related alterations in the modular organization of structural cortical network by using cortical thickness from MRI. Neuroimage 56, 235–245.

Clapp, W.C., Rubens, M.T., Sabharwal, J., Gazzaley, A., 2011. Deficit in switching between functional brain networks underlies the impact of multitasking on working memory in older adults. Proc. Natl. Acad. Sci. U. S. A. 108, 7212–7217.

Cole, M.W., Bassett, D.S., Power, J.D., Braver, T.S., Petersen, S.E., 2014. Intrinsic and task-evoked network architectures of the human brain. Neuron 83, 238–251.

Cohen, J., Cohen, P., West, S.G., Aiken, L.S., 2003. Applied Multiple Regression/Correlation Analysis for the Behavioral Sciences. Erlbaum, Mahwah, NJ.

Cox, R.W., 1996. AFNI: software for analysis and visualization of functional magnetic resonance neuroimages. Comput. Biomed. Res. 29, 162–173.

D'Esposito, M., Deouell, L.Y., Gazzaley, A., 2003. Alterations in the BOLD fMRI signal with ageing and disease: a challenge for neuroimaging. Nat. Rev. Neurosci. 4, 863–872.

Damoiseaux, J.S., Beckmann, C.F., Arigita, E.J.S., Barkhof, F., Scheltens, P., Stam, C.J., Smith, S.M., Rombouts, S.A.R.B., 2008. Reduced resting-state brain activity in the "default network" in normal aging. Cereb. Cortex 18, 1856–1864.

Danon, L., Díaz-Guilera, A., Duch, J., Arenas, A., 2005. Comparing community structure identification. J. Stat. Mech. Theor. Exp. 2005, 09008.

Dehaene, S., Kerszberg, M., Changeux, J.P., 1998. A neuronal model of a global workspace in effortful cognitive tasks. Proc. Natl. Acad. Sci. U. S. A. 95, 14529–14534.

Ferreira, L.K., Busatto, G.F., 2013. Resting-state functional connectivity in normal brain aging. Neurosci. Biobehav. Rev. 37, 384–400.

Funahashi, S., Bruce, C.J., Goldman-Rakic, P.S., 1993a. Dorsolateral prefrontal lesions and oculomotor delayed-response performance: evidence for mnemonic "scotomas". J. Neurosci. 13, 1479–1497.

Funahashi, S., Chafee, M.V., Goldman-Rakic, P.S., 1993b. Prefrontal neuronal activity in rhesus monkeys performing a delayed anti-saccade task. Nature 365, 753–756.

Fuster, J.M., Bauer, R.H., Jervey, J.P., 1985. Functional interactions between inferotemporal and prefrontal cortex in a cognitive task. Brain Res. 330, 299–307.

Gazzaley, A., Cooney, J.W., Rissman, J., D'Esposito, M., 2005. Top-down suppression deficit underlies working memory impairment in normal aging. Nat. Neurosci. 8, 1298–1300.

Gazzaley, A., Nobre, A.C., 2012. Top-down modulation: bridging selective attention and working memory. Trends Cogn. Sci. 16, 128–134.

Geerligs, L., Renken, R.J., Saliasi, E., Maurits, N.M., Lorist, M.M., 2014a. A brain-wide study of age-related changes in functional connectivity. Cereb. Cortex 25, 1987–1999.

Geerligs, L., Saliasi, E., Renken, R.J., Maurits, N.M., Lorist, M.M., 2014b. Flexible connectivity in the aging brain revealed by task modulations. Hum. Brain Mapp. 35, 3788–3804.

Grady, C., 2012. The cognitive neuroscience of ageing. Nat. Rev. Neurosci. 13, 491–505.

Grady, C.L., 2008. Cognitive neuroscience of aging. Ann. N. Y. Acad. Sci. 1124, 127–144.

Guimera, R., Amaral, L.A.N., 2005. Functional cartography of complex metabolic networks. Nature 433, 895–900.

Guimera, R., Sales-Pardo, M., Amaral, L.A.N., 2006. Classes of complex networks defined by role-to-role connectivity profiles. Nat. Phys. 3, 63–69.

Kirkpatrick Jr., S., Gelatt Jr., D., Vecchi, M.P., 1983. Optimization by simulated annealing. Science 220, 671–680.

Kitzbichler, M.G., Henson, R.N.A., Smith, M.L., Nathan, P.J., Bullmore, E.T., 2011. Cognitive effort drives workspace configuration of human brain functional networks. J. Neurosci. 31, 8259–8270.

Knight, R.T., Staines, W.R., Swick, D., Chao, L.L., 1999. Prefrontal cortex regulates inhibition and excitation in distributed neural networks. Acta Psychol. (Amst) 101, 159–178.

Lee, T.G., D'Esposito, M., 2012. The dynamic nature of top-down signals originating from prefrontal cortex: a combined fMRI-TMS study. J. Neurosci. 32, 15458–15466.

Liang, X., Zou, Q., He, Y., Yang, Y., 2015. Topologically reorganized connectivity architecture of default-mode, executive-control, and salience networks across working memory task loads. Cereb. Cortex 26, 1501–1511.

Makris, N., Kennedy, D.N., McInerney, S., Sorensen, A.G., Wang, R., Caviness, V.S., Pandya, D.N., 2005. Segmentation of subcomponents within the superior longitudinal fascicle in humans: a quantitative, in vivo, DT-MRI study. Cereb. Cortex 15, 854–869.

Mattay, V.S., Fera, F., Tessitore, A., Hariri, A.R., Berman, K.F., Das, S., Meyer-Lindenberg, A., Goldberg, T.E., Callicott, J.H., Weinberger, D.R., 2006. Neurophysiological correlates of age-related changes in working memory capacity. Neuroscience 392, 32–37.

Meunier, D., Achard, S., Morcom, A., Bullmore, E., 2009a. Age-related changes in modular organization of human brain functional networks. Neuroimage 44, 715–723.

Meunier, D., Lambiotte, R., Bullmore, E.T., 2010. Modular and hierarchically modular organization of brain networks. Front. Neurosci. 4, 1–11.

Meunier, D., Lambiotte, R., Fornito, A., Ersche, K.D., Bullmore, E.T., 2009b. Hierarchical modularity in human brain functional networks. Front. Neuroinform. 3.

Miller, B.T., D'Esposito, M., 2005. Searching for "the top" in top-down control. Neuron 48, 535–538.

Mori, S., Oishi, K., Jiang, H., Jiang, L., Li, X., Akhter, K., Hua, K., Faria, A.V., Mahmood, A., Woods, R., Toga, A.W., Pike, G.B., Neto, P.R., Evans, A., Zhang, J., Huang, H., Miller, M.I., van Zijl, P., Mazziotta, J., 2008. Stereotaxic white matter atlas based on diffusion tensor imaging in an ICBM template. Neuroimage 40, 570–582.

Myers, L., Sirois, M.J., 2006. Spearman Correlation Coefficients, Differences between. Encyclopedia of Statistical Sciences. John Wiley and Sons, New York, pp. 7901–7902.

Newman, M.E., 2006. Modularity and community structure in networks. Proc. Natl. Acad. Sci. 103, 8577–8582.

Newman, M.E., Girvan, M., 2004. Finding and evaluating community structure in networks. Phys. Rev. E 69, 026113.

Onoda, K., Yamaguchi, S., 2013. Small-worldness and modularity of the resting-state functional brain network decrease with aging. Neurosci. Lett. 556, 104–108.

Park, D.C., Lautenschlager, G., Hedden, T., Davidson, N.S., Smith, A.D., Smith, P.K., 2002. Models of visuospatial and verbal memory across the adult life span. Psychol. Aging 17, 299–320.

Power, J.D., Barnes, K.A., Snyder, A.Z., Schlaggar, B.L., Petersen, S.E., 2012. Spurious but systematic correlations in functional connectivity MRI networks arise from subject motion. Neuroimage 59, 2142–2154.

Power, J.D., Cohen, A.L., Nelson, S.M., Wig, G.S., Barnes, K.A., Church, J.A., Vogel, A.C., Laumann, T.O., Miezin, F.M., Schlaggar, B.L., Petersen, S.E., 2011. Functional network organization of the human brain. Neuron 72, 665–678.

Power, J.D., Mitra, A., Laumann, T.O., Snyder, A.Z., Schlaggar, B.L., Petersen, S.E., 2013. Methods to detect, characterize, and remove motion artifact in resting state fMRI. Neuroimage 84, 1–22.

Reuter-Lorenz, P.A., Cappell, K.A., 2008. Neurocognitive aging and the compensation hypothesis. Curr. Dir. Psychol. Sci. 17, 177–182.

Rorden, C., Bonilha, L., Nichols, T.E., 2007. Rank-order versus mean based statistics for neuroimaging. Neuroimage 35, 1531–1537.

Sadaghiani, S., Poline, J.-B., Kleinschmidt, A., D'Esposito, M., 2015. Ongoing dynamics in large-scale functional connectivity predict perception. Proc. Natl. Acad. Sci. U. S. A. 112, 8463–8468.

Satterthwaite, T.D., Elliott, M.A., Gerraty, R.T., Ruparel, K., Loughead, J., Calkins, M.E., Eickhoff, S.B., Hakonarson, H., Gur, R.C., Gur, R.E., Wolf, D.H., 2013. An improved framework for confound regression and filtering for control of motion artifact in the preprocessing of resting-state functional connectivity data. Neuroimage 64, 240–256.

Smith, S.M., 2002. Fast robust automated brain extraction. Hum. Brain Mapp. 17, 143–155.

Smith, S.M., Jenkinson, M., Johansen-Berg, H., Rueckert, D., Nichols, T.E., Mackay, C.E., Watkins, K.E., Ciccarelli, O., Cader, M.Z., Matthews, P.M., Behrens, T.E.J., 2006. Tract-based spatial statistics: voxelwise analysis of multi-subject diffusion data. Neuroimage 31, 1487–1505.

Smith, S.M., Jenkinson, M., Woolrich, M.W., Beckmann, C.F., Behrens, T.E.J., Johansen-Berg, H., Bannister, P.R., De Luca, M., Drobnjak, I., Flitney, D.E., Niazy, R.K., Saunders, J., Vickers, J., Zhang, Y., De Stefano, N., Brady, J.M., Matthews, P.M., 2004. Advances in functional and structural MR image analysis and implementation as FSL. Neuroimage 23, S208–S219.

Spreng, R.N., Wojtowicz, M., Grady, C.L., 2010. Reliable differences in brain activity between young and old adults: a quantitative meta-analysis across multiple cognitive domains. Neurosci. Biobehav. Rev. 34, 1178–1194.

Stanley, M.L., Dagenbach, D., Lyday, R.G., 2014. Changes in global and regional modularity associated with increasing working memory load. Front. Hum. Neurosci. 8.

Turner, G.R., Spreng, R.N., 2012. Executive functions and neurocognitive aging: dissociable patterns of brain activity. Neurobiol. Aging 33, 826.e1–826.e13.

Turner, G.R., Spreng, R.N., 2015. Prefrontal engagement and reduced default network suppression co-occur and are dynamically coupled in older adults: the default–executive coupling hypothesis of aging. J. Cogn. Neurosci. 27, 2462–2476.

Tzourio-Mazoyer, N., Landeau, B., Papathanassiou, D., Crivello, F., Etard, O., Delcroix, N., Mazoyer, B., Joliot, M., 2002. Automated anatomical labeling of activations in SPM using a macroscopic anatomical parcellation of the MNI MRI single-subject brain. Neuroimage 15, 273–289.

Van Dijk, K.R.A., Sabuncu, M.R., Buckner, R.L., 2012. The influence of head motion on intrinsic functional connectivity MRI. Neuroimage 59, 431–438.

Vatansever, D., Menon, D.K., Manktelow, A.E., Sahakian, B.J., Stamatakis, E.A., 2015. Default mode dynamics for global functional integration. J. Neurosci. 35, 15254–15262.

Wen, X., Zhang, D., Liang, B., Zhang, R., Wang, Z., Wang, J., Liu, M., Huang, R., 2015. Reconfiguration of the brain functional network associated with visual task demands. PLoS One 10, e0132518.

Woolrich, M.W., Jbabdi, S., Patenaude, B., Chappell, M., Makni, S., Behrens, T., Beckmann, C., Jenkinson, M., Smith, S.M., 2009. Bayesian analysis of neuroimaging data in FSL. Neuroimage 45, S173–S186.